Nonlinear dynamics and small damping signal control of chaos in a model of flow-induced oscillations of cylinders

M. Siewe Siewe [a,b,*], X. Xia [b]

[a] Laboratoire de Mécanique, Département de Physique, Faculté des sciences, Université de Yaoundé I, B.P. 812 Yaoundé, Cameroon
[b] Department of Electrical, Electronic and Computer Engineering, University of Pretoria, Pretoria, 0002, South Africa

ARTICLE INFO

ABSTRACT

Nonlinear dynamics of flow-induced oscillations of cylinders is investigated. The approach in our paper is made to introduce an harmonic forced vibration in the coupling term of the structural equation since this may be the consequence of approximating the potential force that could act as a periodic excitation. The method of multiple scales is used to determine the steady state responses. Amplitude and phase modulation equations as well as external force-response and frequency-response curves are obtained. We show that harmonic excitation can induce resonance phenomena in the oscillation of the structure for a range of frequencies of potential force, and also lock-in phenomena appear in the structure part. Also, we find that the structure can be damaged as the amplitude of the potential excitation increases. Numerical simulations confirm the existence of chaotic vibration in the system, a small damping signal control is used to suppress it since it may cause fatigue in the system. The model developed is expected to yield better results for structure in water.

Crown Copyright © 2012 Published by Elsevier Ltd. All rights reserved.

1. Introduction

Vortex-induced vibration (VIV) of cylindrical structures modelled by coupled oscillators has been a subject of extensive theoretical, experimental and numerical studies (Iwan, 1975; Iwan and Blevins, 1974; Williamson and Govardhan, 2004; Sarpkaya, 2004; Gabbai and Benaroya, 2005). Cross wind vibration of slender structures induced by vortex shedding may occur under certain meteorological conditions. This vortex shedding induces an approximately periodic excitation on the structure and causes it to vibrate. The structural vibration modifies the flow, which in turn alters the induced force acting on the cylinder. The resulting fluid–structure interaction is a non-linear process and will give rise to structural vibration with multiple frequencies (Blevins, 1994; Blake, 1986). In extreme cases this may lead to failure of the structures, but even if this event does not occur, the vibrations will cause fatigue damage in the materials of the structure, thereby increasing the maintenance cost of the building. In addition, the excessive acceleration magnification will frequently cause occupants' discomfort (Love and Tait, 2010; Wu et al., 2009). The suppression of these oscillations has become one of the major

concerns to civil engineers. A number of methods exist for improving the performance of existing structures to meet the requirements. Strengthening of the buildings or the installation of a base isolation system is complicated, difficult, and expensive. Therefore, incorporating control devices is proposed to mitigate excessive oscillations. Recently, (Alvarez-Ramirez et al., 2003; Tereshko et al., 2004; De Souza et al., 2007) have shown that the injection of small damping signals suffices to regulate the motion of a chaotic system around less complex attractors, such as equilibrium points and periodic orbits.

A model of VIV failure, is generally taken as a paradigmatic example of the resonance effects on structures under the action of time-periodic forcing caused by vortex shedding due to impinging wind on the structure. Even recognizing that the ultimate source of the problem is the interaction between the periodicities of the structure oscillations and the vortices that are created, it turns out that the standard textbook explanation, based on linear resonance arguments, is somewhat imprecise (Billah and Scanlan, 1991). Linear resonance is a rather narrow phenomenon and very difficult to occur in an irregularly changing environment (Lazer and McKenna, 1990). The possible inadequacy of a linear explanation for the structure in a model of vortex induced vibration to describe response characteristics, such as the amplification of body displacement at lock-in and frequency lock-in, both at high and low mass ratios was already pointed out in the work done by Ref. (Li-ming et al., 2009). Due to advances in the understanding of nonlinear oscillators (Nayfeh and Mook, 1979), the role of nonlinear effects in the dynamical behavior of suspension bridges has been better

* Corresponding author at: Laboratoire de Mécanique, Département de Physique, Faculté des sciences, Université de Yaoundé I, B.P. 812 Yaoundé, Cameroun. Fax: +27 124203893.
  E-mail addresses: martinsiewesiewe@yahoo.fr (M. Siewe Siewe), xxia@postino.up.ac.za (X. Xia).

appreciated. In this perspective, the nonlinear response analysis of vortex-induced vibration in a structure–wake system consisting each of a nonlinear damping oscillators has been considered in Ref. (Li-ming et al., 2009).

Semi-empirical models for VIV of spring-loaded rigid right infinite cylinder have been widely studied (Matsumoto et al., 2001; Chang and Gu, 1999). A review article by Parkinson (Parkinson, 1989) presents a good summary of these models. A van der Pol-type oscillator is commonly used to represent the time varying forces on the structure due to vortex shedding (Bishop and Hassan, 1964). This equation has a negative damping term (energy input) at small motion and a positive damping term (energy dissipation) at larger motion. It is therefore able to model the self-excited and self-limiting nature of VIV. However, this model is still unsatisfactory for predicting quantitatively the transition region in the parameter space (Plaschko, 1996). Hence, a modified version of semi-empirical model equations has been proposed, where the transition of flow-induced vibrations to chaos in terms of heteroclinic bifurcation were investigated.

Among all researchers mentioned above, only the free vibration experimental and theoretical is considered. In their work (Ogink and Metrikine, 2010), an attempt has been made to improve a wake oscillator model based on the model of Facchinetti et al. (Facchinetti et al., 2004). By introducing a frequency dependent coupling. The idea of this improvement arises from the obvious desire to have a model that satisfies both the free and forced vibration experiments. To extend research in this area of forced vibration, this paper investigates the nonlinear oscillations and chaos control in a structure–wake system with external periodic excitation due to the potential force. The resulting governing equations of motion describe a two-degree-of-freedom system having cubic nonlinearities and external excitation. Our goal in this paper is twofold. First, the effect of the forced excitation on the nonlinear response is studied. On the other hand, chaotic vibration due to forced excitation is controlled. The method of multiple time scales perturbation technique is used to solve the nonlinear differential equations describing the response system up to second order accuracy. The case of mixed resonance and effects of system's various parameters are studied numerically. Chaos control using small amplitude damping signals is used to suppress the chaotic oscillation of the system.

2. Description of the vortex induced-vibrations on a spring-loaded rigid right infinite cylinder

Even though a considerable number of structure–wake oscillator models have been developed, the correspondence between model predictions and VIV measurements is in most cases adequate at best. The main problem is to find a model that can describe at the same time both the correct range of flow velocities, in which lock-in takes place, and the correct amplitude of cylinder motion. Here, we assume that the structural elasticity includes cubic nonlinearity. In the literature, so many different phenomenological forcing terms have been used to model the coupling function between the structure and wake oscillator. It has been shown in Ref. (Li-ming et al., 2009) that the coupling term in the structure equation includes the potential force $F_{potential} = -m_f \ddot{y}$, where m_f is the potential fluid-added mass, and the vortex force F_{vortex}. In Ref. (Li-ming et al., 2009), the potential force was neglected to consider only the vortex force. In our case, to improve the concept of the oscillator model it is proposed to make the coupling term in the structure equation frequency dependent (i.e., to consider that the potential force can be approximated by a small harmonic function of time with frequency ω). The fluid oscillator and the interaction between the structure and the flow are modelled in the same manner in Ref. (Gabbai and

Benaroya, 2005), but a time varying coupling term is added and imposed on the structure. We propose the following model of the vortex induced-vibrations on a bridge column

$$\ddot{x} + 2\tilde{\mu}\dot{x} + \omega_1^2 x + \tilde{\nu}x^3 = \tilde{\gamma}_1 y + \tilde{f}_0 \cos \omega t, \tag{1}$$

$$\ddot{y} - (\tilde{\alpha} - \tilde{\beta}\dot{y}^2)\dot{y} + \omega_2^2 y = \tilde{\gamma}_2 \dot{x}, \tag{2}$$

In the above equations, x is the dimensionless spring-loaded rigid right infinite cylinder displacement and y is a representative fluid property, for example, pressure or lift coefficient on the structure. $\gamma_1 y + f_0 \cos \omega t$, and $\gamma_2 \dot{x}$ model the coupling between lift force and structure motion. The dots represent differentiation with respect to time t, ω_i are the free frequencies of the structure and fluid and $\tilde{\alpha}$, $\tilde{\beta}$, $\tilde{\mu}$, $\tilde{f}_0$, $\tilde{\nu}$, $\tilde{\gamma}_1$, and $\tilde{\gamma}_2$ are positive constants. Here the structure is modelled by a forced and damped nonlinear oscillator (Eq. (1)), while the periodic vortex shedding on the fluid is modelled by a Rayleigh oscillator (Eq. (2)).

3. Perturbation solution

In this section, we use the method of multiple scales (Nayfeh and Mook, 1979) to find the averaged equations of the system. Our aim here is that one would expect a coupled nonlinear oscillator to exhibit (approximately) oscillations which occur at the external and mixed resonance depending of the magnitude of the external amplitude f_0. In this section, the damping, nonlinear and coupling coefficients are considered as global first order perturbations and then may be rewritten as $\tilde{\alpha} = \varepsilon\alpha$, $\tilde{\beta} = \varepsilon\beta$, $\tilde{\mu} = \varepsilon\mu$, $\tilde{f}_0 = \varepsilon f_0$, $\tilde{\nu} = \varepsilon\nu$, $\tilde{\gamma}_1 = \varepsilon\gamma_1$, and $\tilde{\gamma}_2 = \varepsilon\gamma_2$. To this end, we introduce a fast time scale $T_0 = t$ and a slow time scale $T_1 = \varepsilon t$ where ε is a small dimensionless parameter. Then, the time derivative become

$$\begin{cases} \dfrac{d}{dt} = D_0 + \varepsilon D_1 + ..., \\ \dfrac{d^2}{dt^2} = D_0^2 + 2\varepsilon D_0 D_1 + ... \end{cases} \tag{3}$$

where the differentiation operator $D_k = \partial/\partial T_k$, $k = 0, 1$.

The expression of $x(t; \varepsilon)$ and $y(t; \varepsilon)$ are taken to be in the form

$$\begin{cases} x(t; \varepsilon) = x_0(T_0, T_1) + \varepsilon x_1(T_0, T_1) + ..., \\ y(t; \varepsilon) = y_0(T_0, T_1) + \varepsilon y_1(T_0, T_1) + ... \end{cases} \tag{4}$$

Substituting solution (4) into system Eqs. (1) and (2) with all the above new parameters, then dropping the tildes on terms, and balancing the coefficients of like powers of ε in the resulting equation yields the following ordered perturbation equations:

Order ε^0:

$$\begin{cases} D_0^2 x_0 + \omega_1^2 x_0 = 0, \\ D_0^2 y_0 + \omega_2^2 y_0 = 0. \end{cases} \tag{5}$$

Order ε^1:

$$\begin{cases} D_0^2 x_1 + \omega_1^2 x_1 = -2D_0 D_1 x_0 - 2\mu D_0 x_0 + \gamma_1 y_0 - \nu x_0^3 + f_0 \cos \omega T_0 \\ D_0^2 y_1 + \omega_2^2 y_1 = -2D_0 D_1 y_0 + \left(\alpha - \beta(D_0 y_0)^2\right) D_0 y_0 + \gamma_2 D_0 x_0. \end{cases} \tag{6}$$

The general solutions of system Eq. (5) can be expressed as

$$\begin{cases} x_0 = A(T_1) \exp j\omega_1 T_0 + c.c, \\ y_0 = B(T_1) \exp j\omega_2 T_0 + c.c, \end{cases} \tag{7}$$

where $c.c.$ stands for complex conjugate of its preceding terms. The functions A and B are unknown function of T_1 and $j = \sqrt{-1}$; their dependence on time will be exhibited when solving the solvability conditions. Substituting the solutions x_0 and y_0 into the right-hand

side of Eq. (6) yields an expression in terms of trigonometric functions as follows

$$D_0^2 x_1 + \omega_1^2 x_1 = -j\left(2\omega_1\dot{A} + 2\mu\omega_1 A + 3\nu \mid A\mid^2 A\right)\exp j\omega_1 T_0$$

$$+ \gamma_1 B\exp j\omega_2 T_0 - \nu A^3\exp 3j\omega_1 T_0 \qquad (8)$$

$$+ \frac{f_0}{2}\exp j\omega T_0 + c.c$$

$$D_0^2 y_1 + \omega_2^2 y_1 = j\omega_2\left(-2\dot{B} - 3\omega_2^2\beta \mid B\mid^2 B + \alpha B\right)\exp j\omega_2 T_0$$

$$+ j\beta\omega_2^3 B^3\exp 3j\omega_2 T_0 + j\gamma_2\omega_1 A\exp j\omega_1 T_0 + c.c \qquad (9)$$

where the dot on A and B denotes the differentiation with respect to T_1. They can be determined by eliminating the secular terms at the next approximation. From the above Eqs. (8) and (9), the resonance cases are: external resonance ($\omega = \omega_1$); internal resonance ($\omega_2 = \omega_1$); simultaneous resonance, i.e., any combination of the above resonance cases is considered as a simultaneous resonance. In this paper, only the last case of simultaneous resonance will be analyzed because it is the one that couples the structure with the wake and also gives the effect of the harmonic excitation on the steady state oscillation.

3.1. The mixed resonance case

Here, we analyze the case where the structure inters in an external resonance with the harmonic excitation ($\omega = \omega_1$) in the presence of one-to-one internal resonance ($\omega_1 = \omega_2$). The previous resonant relations can be expressed as follows

$$\omega_1 = \omega_2 + \varepsilon\sigma_1, \qquad \omega = \omega_1 + \varepsilon\sigma_0 \qquad (10)$$

where σ_0 measures the detuning between the excitation frequency and the natural frequency of the first oscillator, σ_1 gives a measure of the internal detuning between the two oscillators. Substituting (10) into Eqs. (8) and (9) together with the polar representations below

$$\begin{cases} A = \dfrac{a(T_1)}{2}\exp j\theta_1(T_1) + c.c, \\[2mm] B = \dfrac{b(T_1)}{2}\exp j\theta_2(T_1) + c.c, \end{cases} \qquad (11)$$

where a, b and θ_1, θ_2 are respectively the amplitudes and phases of the oscillators. The secular producing terms in Eqs. (8) and (9) must be eliminated. Using the solvability conditions and after separating real and imaginary parts, the following set of first-order differential equations is obtained:

$$\begin{cases} \omega_1\dot{a} + \mu\omega_1 a + \dfrac{3\nu}{8}a^3 - \dfrac{\gamma_1}{2}b\sin\delta_1 - \dfrac{f_0}{2}\sin\delta_0 = 0, \\[2mm] \omega_1 a\left(\sigma_0 - \dot{\delta}_0\right) + \dfrac{\gamma_1}{2}b\cos\delta_1 + \dfrac{f_0}{2}\cos\delta_0 = 0, \\[2mm] \omega_2\dot{b} + \dfrac{3\omega_2^3\beta}{8}b^3 - \dfrac{\alpha\omega_2}{2}b - \dfrac{\gamma_2\omega_1}{2}a\cos\delta_1 = 0, \\[2mm] b\omega_2(\dot{\delta}_1 - \dot{\delta}_0) + b\omega_2(\sigma_0 + \sigma_1) + \dfrac{\gamma_2\omega_1}{2}a\sin\delta_1 = 0, \end{cases} \qquad (12)$$

where $\delta_0 = \sigma_0 T_1 - \theta_1$, and $\delta_1 = \theta_2 - \theta_1 - \sigma_1 T_1$.

The singular points of system Eq. (12) corresponding to steady state and periodic equilibrium are described by assuming $\dot{a} = \dot{b} = 0$ and $\dot{\delta}_1 = \dot{\delta}_0 = 0$. Using these conditions in system Eq. (12) leads to the following set of nonlinear algebraic equations that are solved numerically to obtain the fixed point response of the system

$$a^2 = \frac{4\omega_2^2(\sigma_0 + \sigma_1)^2}{\gamma_2^2\omega_1^2}b^2 + \frac{\omega_2^2 b^2}{\gamma_2^2\omega_1^2}\left(\alpha - \frac{3\beta\omega_2^2}{4}b^2\right)^2, \qquad (13)$$
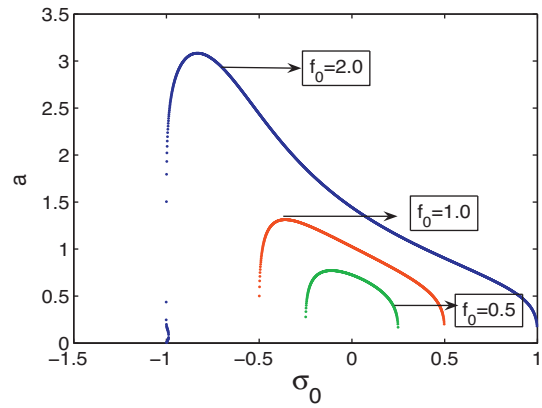
Fig. 1. Frequency response curve on the structure for different excitation amplitude.

and

$$\left(\omega_1^2\gamma_2\sigma_0 a^2 + \frac{\gamma_1\omega_2}{2}\left(\frac{3\beta\omega_2^2}{4}b^2 - \alpha\right)b\right)^2$$

$$+\left(\gamma_1\omega_2(\sigma_0 + \sigma_1)b^2 + \gamma_2\omega_1\left(\mu\omega_1 + \frac{3\nu}{8}a^2\right)a^2\right)^2 \qquad (14)$$

$$-\frac{f_0^2\omega_1^2\gamma_2^2 a^2}{4} = 0$$

4. Frequency and forced response curves

In this section, the fixed point response of the coupled oscillators is obtained by solving the frequency response Eqs. (13) and (14) numerically for fixed parameters $\mu = 0.0015$, $\nu = 0.05$, $\alpha = 0.002$, $\beta = 0.067$, $\gamma_1 = 0.002$, $\gamma_2 = 0.4$, $\sigma_1 = 1$, $\omega_1 = 1$, and $\omega_2 = 1$. The representative solutions are illustrated by the frequency and forced responses plots of Figs. 1 and 2.

In Fig. 1, a typical frequency-response graph is shown. The steady-state response of the structure plot given in Fig. 1 shows the resonant of a system for three values of the amplitude of external excitation. The physical consistency of the modeling can be verified by three values of the amplitude of the external excitation. Increasing amplitude excitation is found to enlarges the lock-in domain and progressively increase the resonance peak. Meanwhile, dotted line appearing in Fig. 1 characterize unstable solutions. Therefore, this property enables one to design an appropriate external amplitude to enhance the control performance and avoid the appearance
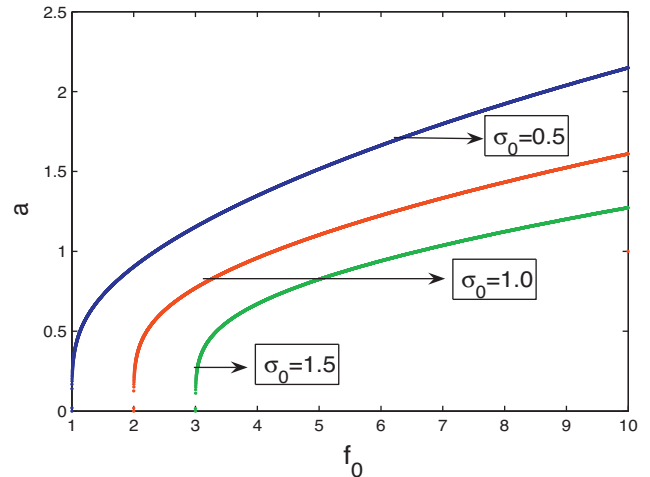
Fig. 2. Forced response curve on the structure for different detuning parameter.
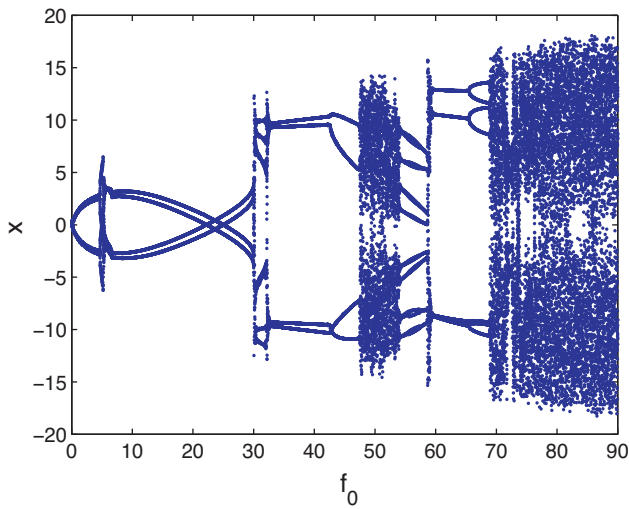
Fig. 3. Bifurcation diagram of the structure showing the projections of the attractors in the stroboscopic section against the external excitation amplitude f_0. $\mu = 0.0015$, $\nu = 0.05$, $\alpha = 0.002$, $\beta = 0.067$, $\gamma_1 = 0.002$, $\omega_2 = \omega_1 = 1$, $\omega = 0.75$ and $\gamma_2 = 0.4$.

of the higher amplitude oscillation in practical vibration control. Fig. 2 presents the forced response of the system, under the effect of the detuning parameter. From this figure, it is shown that for a fixed value of the detuning parameter σ_0, there is one solution whose amplitude increases and tend asymptotically to a non-zero amplitude value as the amplitude of the potential force increases. The above forced response curve can be used to control the vibration of the structure, in fact, it is easy to see that when the value of the detuning parameter tends to zero then the structure will oscillate with higher amplitude and consequently, the structure will be damaged.

5. Chaotic dynamics of the coupled oscillators

The aim of this section is to use numerical simulations to establish parameter regimes where specific behavior of our model of vortex-induced vibration could be expected, and thus to determine for which parameter combinations either periodic, quasi-periodic or chaotic behavior could be avoided or encountered. In the two-time scales analysis in Section 4, most coefficients of (1) and (2) are assumed small and of the same order. However, it is interesting to know the dynamics of the system when the parameters vary in different ranges. In this section, the dependence of the system dynamics on its parameters is studied using a bifurcation analysis. The internal resonance condition $\omega_1 = \omega_2$ is applied. Sometimes, it is easy to adjust the driving force to change the behavior of the coupled system once it is designed and physically constructed. Therefore, the frequency and amplitude of the driving force are used as main control parameters in the bifurcation. The diagnostics used to establish structural changes involved, bifurcation diagrams in the intervals of the amplitude of the external forcing f_0 and the influence of the f_0 in the Poincaré maps. The fourth-order Runge–Kutta routine is used for numerical integration. The bifurcation diagrams for specific parameter values are presented in Fig. 3 for $0 \le f_0 \le 90$.

It is shown from Fig. 3 that the structure behavior in a fundamentally periodic and weak chaotic solutions persisting for $f_0 \le 31$. At the value of $f_0 = 31$, a period-4 until the value $f_0 \approx 47.5$. At the value of $f_0 \succ 47.5$, until 53.6, a first large band chaotic solution is born and as f_0 increases the system undergoes multi-periodic, weak chaotic and a successively period doubling solutions. A chaotic-saddle explosion appears at $f_0 \approx 67$. Here, the chaotic attractor undergoes an abrupt instantaneous enlargement to a larger chaotic
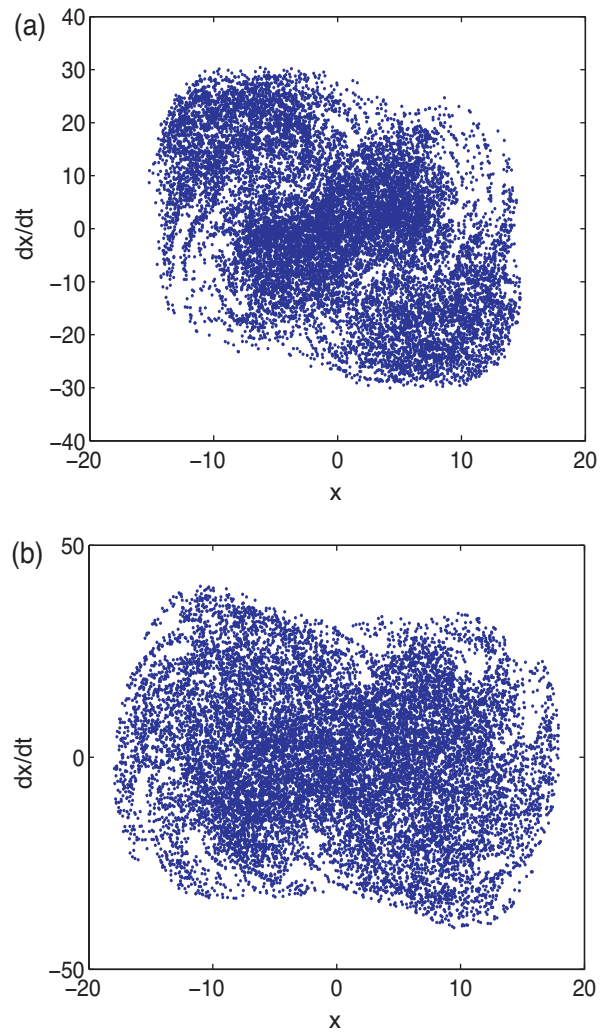
Fig. 4. Poincaré maps (a) $f_0 = 52$ (b) $f_0 = 85$.

attractor, which includes the original attractor as a subset, on colliding with a chaotic saddle.

The qualitative change on the system dynamics due to the amplitude of the parametric perturbation is examined on the Poincaré maps whose attractor geometrical structure looks very complicated. As the control parameter f_0 becomes smaller, the number of the fixed points in cluster decreases and the fractal structure of the attractor becomes more and more visible as shown in Fig. 4(a). The following investigation is motivated by the fact that a small amplitude damping suffices to regulate the motion of the coupled chaotic system around less complex attractors, such as equilibrium points and periodic orbits. By a small damping force, we mean that chaos suppression can be obtained with controllers using small energy levels compared with the total energy of the system. This is the aim of the next section.

6. Small damping signal control of chaos

In this section, the focus is shifted to the suppression of chaotic motion in the vortex induced-vibration (VIV) system. To do so, we can add a control input in Eqs. (1) and (2) in the following form

$$
\begin{cases}
\ddot{x} + 2\mu\dot{x} + \omega_1^2 x + \nu x^3 = \gamma_1 y + f_0 \cos \omega t + u(\dot{x}), \\
\ddot{y} - (\alpha - \beta \dot{y}^2)\dot{y} + \omega_2^2 y = \gamma_2 \dot{x},
\end{cases}
\tag{15}
$$
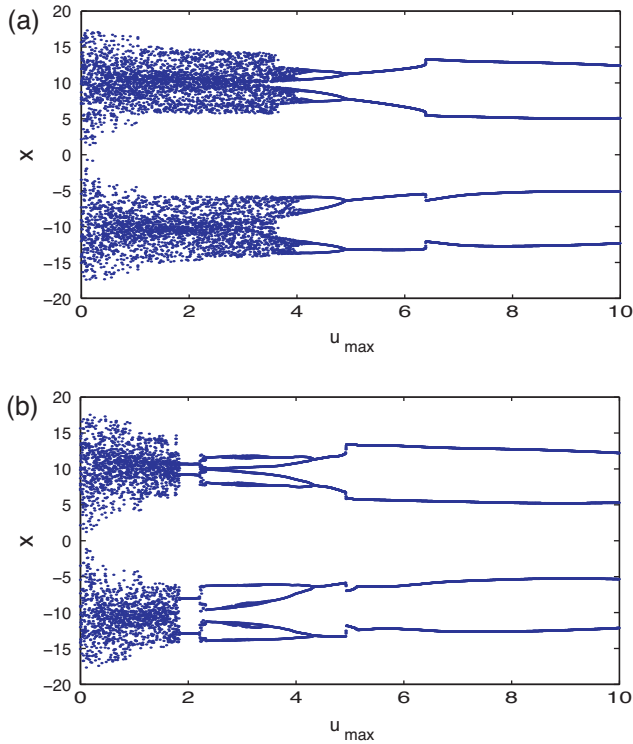
Fig. 5. Bifurcation diagrams of the cylinder in terms of control parameters showing the suppressing of the chaotic attractors of Fig. 4(a) in the stroboscopic section into (a)–(c) $k_e = 0.4$, $\tau = 0.2$ and (b)–(d) $k_e = 5$, $\tau = 0.2$ against the control parameter u_{max} for $f_0 = 85$.

where u is the control signal needed to be chosen. It should be stressed that the control input could be a liquid lubricant or a damping force acting on the spring-loaded rigid right infinite cylinder. Since system (15) can be seen as the interconnection between two second-order subsystems in x and y, we conjecture that if we able to suppress the chaotic behavior in the first oscillator, the chaotic motion in the second oscillator will be suppress automatically. This is why, in the sequel, we only consider the following second-order subsystem

$$\ddot{x} + 2\mu\dot{x} + \omega_1^2 x = s(t) + u, \qquad (16)$$

where $s(t) = -\nu x^3 + \gamma_1 y + f_0 \cos \omega t$ is a forcing function which is unknown to us. An alternative to suppress chaos in system equation (15) is to suppress the unceasing interactions of the potential energy with the kinetic energy by introducing a damping action. This can be achieved by a feedback u in terms of the velocity $\dot{x}$:

$$u = -k_e \dot{x}, \qquad (17)$$

where k_e is a positive constant. Then, the resulting controlled system is

$$\ddot{x} + (2\mu + k_e)\dot{x} + \omega_1^2 x = s(t). \qquad (18)$$

Let us consider the following partial energy as a Lyapunov candidate function:

$$E_p(x, \dot{x}) = \frac{1}{2}\dot{x}^2 + \frac{\omega_1^2}{2}x^2. \qquad (19)$$

Its time derivative along the trajectories of the closed-loop system (15) satisfies

$$\dot{E}_p(x, \dot{x}) = -(2\mu + k_e)\dot{x}^2 + \dot{x}s(t). \qquad (20)$$

Let the function $s(t)$ satisfy $|s(t)| \leq s_m$ for some $s_m > 0$.

$$\dot{E}_p(x, \dot{x}) \leq -|\dot{x}| \left\{ (2\mu + k_e)|\dot{x}| - s_m \right\}. \qquad (21)$$

Let us define $D = 1/(2\mu + k_e)$. From inequality (21), it follows that if $|\dot{x}| \geq Ds_m$, then $\dot{E}_p(x, \dot{x}) < 0$, hence, $E_p(x, \dot{x})$ decreases, which implies that $|\dot{x}|$ decreases as well, see inequality (21). It then follows from the standard invariance arguments that the velocity satisfies the following bound:

$$|\dot{x}| \leq c, \qquad (22)$$

where $c \geq Ds_m$, (see Khalil, 1992, p. 323). From inequality (22), it follows that the velocity depends linearly on the constant s_m. Hence, if this term is small, the resulting velocity will be small as well. The dependence of the velocity on k_e deserves special attention. Note that $D = 1/(2\mu + k_e)$. Hence, as k_e increases, $(2\mu + k_e)$ will increase and consequently D will decrease, which also decreases the velocity bound. This argument shows that with the proposed method, k_e should be made as large as possible. In this way, the feedback term u increases the stability properties of the controlled system around equilibrium points.

The feedback function (17) can lead to excessively large control actions, which cannot be available in practice. In practice, in the chaotic systems, the trajectories move erratically but in the bounded region, and hence, require a bounded energy to be stabilized. To avoid this situation, and since the dynamics of the chaotic system are constrained to evolve within a bounded region, we propose the following bounded feedback function:

$$u = -u_{max} \tanh(k_e \dot{x}), \qquad (23)$$

where u_{max} defines the maximum amplitude of the control action.

Once again, the implementation of the damping feedback controller (23) requires measurements of the velocity $v = \dot{x}$. Velocity measurements are not easy because of high noise sensitivity of measurement devices. An alternative is to estimate the velocity $v(t)$ from measurements of the signal $x(t)$. Thus, for the actual velocity $v(t)$, an estimate $v_e(t)$ is obtained as follows:

$$v_e(t) = \frac{s}{\tau_e s + 1}x(t) \qquad (24)$$

where $s = d/dt$ is a time-derivative operator, so that $v = sx$ and $\tau_e > 0$ is a time-constant of the filter. The following must be pointed out. On the one hand, $1/(\tau_e s + 1)$ is a law pass filter with cutting frequency τ_e^{-1} and the operation $(1/(\tau_e s + 1))x(t)$ filters out those dynamics with frequencies significantly larger τ_e^{-1}. In this way, the operation $(s/(\tau_e s + 1))x(t)$ provides a smoother estimate of the time-derivative $\dot{x}$. That is, the larger the time-constant τ_e, the smoother the velocity estimate $v_e(t)$. On the other hand, (24) is equivalent to the differential system $\tau_e \dot{v}_e + v_e = \dot{x}$. Now, let us introduce the variable $\omega_e = \tau_e v_e - x$, so that $v_e = \tau_e^{-1}(\omega_e + x)$. In this way, the velocity estimator (24) is equivalent to the following stable system:

$$\begin{cases} \dot{\omega}_e = -\tau_e^{-1}(\omega_e + x), \\ v_e = \tau_e^{-1}(\omega_e + x). \end{cases} \qquad (25)$$

In this way, the practical feedback control is

$$u = -u_{max} \tanh(k_e v_e). \qquad (26)$$

The robust damping feedback control (26) has the following advantages. (i) It does not require the specification of any reference signal to be tracked by the controlled system. In this case, the feedback strategy (26) can be seen as a self-controlling strategy because it is driven only by measured system signals (Chen et al., 2000). (ii) It only uses the estimate of the velocity $\dot{x}$ which only requires measurements of the signal $x(t)$. (iii) The u_{max}, k_e, τ_e-parametrization of the feedback controller (26) provides a simple tuning procedure. In fact, the control amplitude u_{max} is determined by the capacities
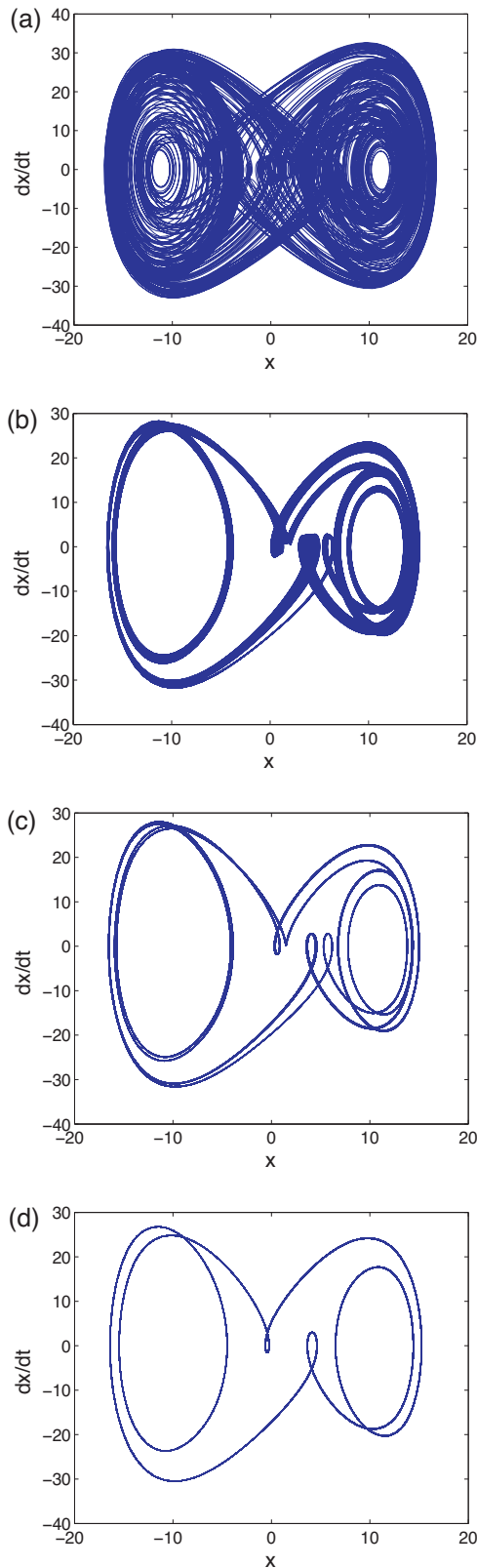
Fig. 6. Phase portrait of the cylinder displacement in terms of the control parameters for $k_e = 0.4$, $\tau = 0.2$ and $f_0 = 85$ (a) $u_{max} = 2$, (b) $u_{max} = 4.2$, (c) $u_{max} = 4.6$, (d) $u_{max} = 6$.

of the control mechanisms. From Eq. (26), one can see that if u_{max} increases, the system trajectories can be less erratic. On the other hand, the control gain k_e determines the aggressiveness of the control action. As k_e is set to large values $u_{max} \tanh(k_e v_e) \simeq u_{max} sign(v_e)$ and the controller injects the maximum damping $\pm u_{max}$. Maybe the most interesting tuning parameter is the filter gain τ_e that determines the smoothness of the velocity estimation.

For the sake of illustration, the time-constant of the filter $\tau = 0.2$ was chosen. In the following the effect of the maximum amplitude u_{max} of the control action on the behavior of the coupled nonlinear oscillators for two value of the control gain k_e will be described. We have plotted in Fig. 5, the bifurcation diagrams for $k_e = 0.4$ and $k_e = 5$. Fig. 5(a) and (b) show that the threshold of chaos to be suppressed in term of u_{max} decrease as as the control gain k_e increases. It is seen from Fig. 5(a) that when we fix $k_e = 0.4$, chaotic behavior appears for $u_{max} \leq 4.1$, while for $4.1 < u_{max} \leq 4.9$ we have a succession of period doubling oscillations, then a range of period-4 oscillations appears for $0.49 < u_{max} \leq 10$ which proves that chaotic vibration is suppressed. At the same time for $k_e = 5$, the region where chaotic behavior appear is $u_{max} \leq 2$, then for $2 < u_{max} \leq 10$ we have a succession of periodic, quasi-periodic and again periodic oscillations. Thus, the chaotic vibration is also suppressed and we only have periodic oscillation. It should be noted that these results are numerically valid when $\tau \leq k_e$. Fig. 6 shows the deformation of the attractor as the parameter u_{max} increases for the control gain $k_e = 0.4$. As expected, more damping is added as u_{max} increases, so the formerly chaotic trajectories are ordered around simpler periodic orbits.

7. Conclusion

In this paper, we have studied the effect of potential force in vortex-induced vibration modelled by a harmonic excitation on the nonlinear dynamics of structure–wake oscillators. Besides their engineering application, structure–wake systems enjoy also a more fundamental interest due to the loss of smoothness in their dynamics, leading to a plethora of complex dynamical phenomena, some of which were presented throughout this paper. We have seen that harmonic excitation can induce resonance phenomena in the oscillation of the structure for a range of frequencies of potential force, while lock-in phenomena also appear in the structure part. Also, we found that the structure can be damaged as the amplitude of the potential excitation increases. On the other hand, the application of a self-controlling feedback has been used in order to reduce the instability effects of chaotic trajectories, leading to a more ordered system evolution. A procedure to suppress chaotic behavior based on small-damping signals has also been presented. This method is based on the fact that by altering the averaged energy of the coupled oscillator, one can steer the system trajectories from chaotic attractor to a periodic orbit which gives improved system performance. This small-damping controller feedback has been confirmed numerically.

Acknowledgement

References

Alvarez-Ramirez, J., Espinosa-Paredes, G., Puebla, H., 2003. Chaos control using small-amplitude damping signals. Physics Letters A 316, 196–205.

Billah, K.Y., Scanlan, R.H., 1991. Resonance, Tacoma Narrows bridge failure, and undergraduate physics textbooks. American Journal of Physics 59, 118–124.

Bishop, R.E.D., Hassan, A.Y., 1964. The lift and drag forces on a circular cylinder oscillating in a flow field. Proceedings of the Royal Society, Series A 277, 32–75.

Blake, W.K., 1986. Mechanics of Flow-Induced Sound and Vibration. New York, Academic.

Blevins, R.D., 1994. Flow-Induced Vibration, 2nd ed. Krieger, New York.

Chang, C.C., Gu, M., 1999. Suppression of vortex-excited vibration of tall buildings using tuned liquid dampers. Journal of Wind Engineering and Industrial Aerodynamics 83, 225–237.

Chen, G., Moiola, J.L., Wang, H.O., 2000. Bifurcation control: theories, methods and applications. International Journal of Bifurcation and Chaos 10, 511–518.

De Souza, S.L.T., Caldas, I.L., Viana, R.L., Balthazar, J.M., Brasil, R.M.L.R.F., 2007. A simple feedback control for a chaotic oscillator with limited power supply. Journal of Sound and Vibration 299, 664–671.

Facchinetti, M.L., De Langre, L., Biolley, F., 2004. Coupling of structure and wake oscillators in vortex-induced vibrations. Journal of Fluids Structures 19, 123–140.

Gabbai, R.D., Benaroya, H., 2005. An overview of modeling and experiments of vortex-induced vibration of circular cylinders. Journal of Sound and Vibration 282, 575–616.

Iwan, W.D., Blevins, R.D., 1974. A model for vortex-induccd oscillation of structures. Journal of Applied Mechanics 41, 581–586.

Iwan, W.D., 1975. The vortex induced oscillation of elastic structural elements. Journal of Engineering, for Industries, Transactions of the American Society of Mechanical Engineers 97, 389–447.

Khalil, H.K., 1992. Nonlinear Systems. Macmillan, New York.

Lazer, A.C., McKenna, P.J., 1990. Large amplitude periodic oscillations in suspension bridges: some new connections with nonlinear analysis. SIAM Review 58, 537–578.

Li-ming, L., Guo-can, L., Ying-xiang, W., Xiao-hui, Z., 2009. Nonlinear fluid damping in structure–wake oscillators in modeling vortex-induced vibrations. Journal of Hydrodynamics 21, 1–11.

Love, J.S., Tait, M.J., 2010. Nonlinear simulation of a tuned liquid damper with damping screens using a modal expansion technique. Journal of Fluids and Structures 26, 1058–1077.

Matsumoto, M., Yagi, T., Shigemura, Y., Tsushima, D., 2001. Vortex-induced cable vibration of cable-stayed bridges at high reduced wind velocity. Journal of Wind Engineering and Industrial Aerodynamics 89, 633–647.

Nayfeh, A.H., Mook, D.T., 1979. Nonlinear Oscillations. John Wiley and Sons, New York.

Ogink, R.H.M., Metrikine, A.V., 2010. A wake oscillator with frequency dependent coupling for the modeling of vortex-induced vibration. Journal of Sound and Vibration 329, 5452–5473.

Parkinson, G.V., 1989. Phenomena and modelling of flow-induced vibrations of bluff bodies. Progress in Aerospace Science 26, 169–224.

Plaschko, P., 1996. Heteroclinic bifurcations in flow-induced oscillations of cylinders. Journal of Fluids and Structures 10, 35–45.

Sarpkaya, T., 2004. A critical review of the intrinsic nature of vortex-induced vibrations. Journal of Fluids and Industrial Structures 19, 389–447.

Tereshko, V., Chacon, R., Preciado, V., 2004. Controlling chaotic oscillators by altering their energy. Physics Letters A 320, 408–416.

Williamson, C., Govardhan, R., 2004. Vortex-induced vibrations. Annual Review of Fluid Mechanics 36, 413–455.

Wu, J.C., Chang, C.H., Lin, Y.Y., 2009. Optimal designs for non-uniform tuned liquid column dampers in horizontal motion. Journal of Sound and Vibration 326, 80–97.